

## **NOTICE CONCERNING COPYRIGHT RESTRICTIONS**

This document may contain copyrighted materials. These materials have been made available for use in research, teaching, and private study, but may not be used for any commercial purpose. Users may not otherwise copy, reproduce, retransmit, distribute, publish, commercially exploit or otherwise transfer any material.

The copyright law of the United States (Title 17, United States Code) governs the making of photocopies or other reproductions of copyrighted material.

Under certain conditions specified in the law, libraries and archives are authorized to furnish a photocopy or other reproduction. One of these specific conditions is that the photocopy or reproduction is not to be "used for any purpose other than private study, scholarship, or research." If a user makes a request for, or later uses, a photocopy or reproduction for purposes in excess of "fair use," that user may be liable for copyright infringement.

This institution reserves the right to refuse to accept a copying order if, in its judgment, fulfillment of the order would involve violation of copyright law.

John F. Schatz  
Terra Tek  
Salt Lake City, Utah

ABSTRACT

This paper describes the results of a project funded by the Lawrence Berkeley Laboratory's Geothermal Subsidence Research Project (which was, in turn, funded by the U.S. Department of Energy's Division of Geothermal Energy). The objectives of the work described here were to acquire cores and fluids from the Cerro Prieto geothermal reservoir, to test those cores for their short-term and long-term (creep) compaction response; and to develop a compaction constitutive model that would allow mathematical models to be subsequently used to predict reservoir compaction and surface subsidence for actual field occurrences.

1. INTRODUCTION

1.1 Background

The withdrawal of fluids in large quantities from surface reservoirs, and subsequent pore pressure reduction, create the potential for reservoir compaction and in turn, the possibility of surface subsidence. Subsidence has been observed in the past at many locations in the world in association with both water and oil withdrawal (see, for example, Grimsrud, et al., 1978). More recently, subsidence has been identified as a possible consequence of hydrothermal fluid production from geothermal reservoirs. For example, at Mexico's Cerro Prieto geothermal field hot brines are produced from a geologically young sedimentary sequence of sands and shales, and cooler fluids may be reinjected. The compaction of the subsurface aquifer and layers above, as caused by fluid pressure reduction, may propagate to the surface in the form of subsidence and may affect natural or man-made agricultural drainage systems.

It can be seen from this background discussion that it is desirable to have a method of understanding and predicting subsidence in geothermal areas. Because of the lacks of widespread historical experience, it is extremely unlikely that an accurate empirical model can be developed in the near future. Consequently, a logical first step (aside from gathering as much field information as possible) is to investigate the physical mechanisms of compaction in geothermal reservoir rocks as caused by

pore pressure reduction.

1.2 Project Plan.

A flow chart of the project, as planned, is shown in Figure 1. Two major legs of the project started simultaneously. One leg began with obtaining core from known and developing geothermal areas.

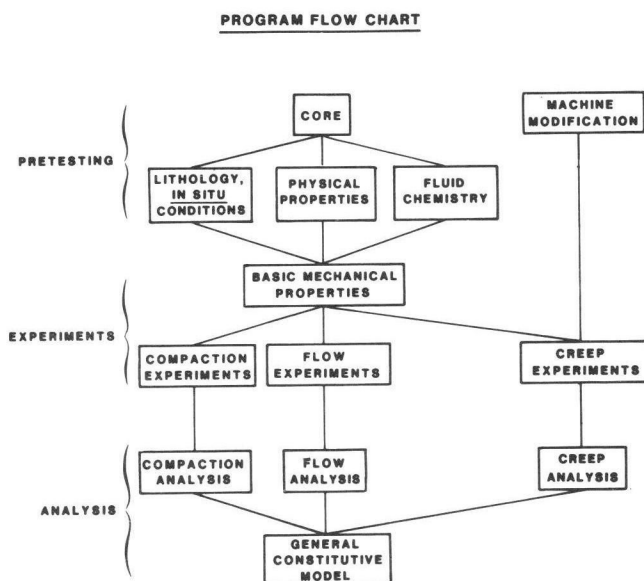


Figure 1. Flow chart showing planned progress of program.

The other leg began with test machine modification to prepare equipment for creep compaction experiments, since the possibility of time-dependent effects at geothermal reservoirs temperatures was considered important enough to warrant study.

Through discussion and cooperation with the Lawrence Berkeley Laboratory the U.S. Department of Energy, and the Comisión Federal de Electricidad of México. Core was brought to the laboratory where lithology, and properties such as density and porosity were determined. Then, work entered into a testing phase for basic mechanical properties with emphasis on measurements of compressibility at reservoir conditions. With basic measurements completed, three types of experiments were performed and data began to be collected

These consisted of compaction experiments, where reservoir conditions were achieved, and materials were caused to compact by reduction of pore pressure; flow experiments, where reservoir conditions were achieved, pore pressure was reduced, and effects on permeability were investigated; and creep experiments on the modified test machine, where reservoir conditions were achieved, pore pressure was reduced and then held at a reduced value for long periods of time (up to several weeks) in order to look at time-dependent effects.

As data became available, work began on analysis for all of these experiments. Ultimately, all data and analyses were brought together to generate a general understanding of the behavior of rocks from these geothermal reservoirs. Theoretical work was undertaken to develop methods of extrapolation of creep behavior to long periods of time. A summary of the results of this work is included in this paper. A complete description of all techniques and results is given by Schatz (1982).

## 2. DESCRIPTION OF MATERIALS

### 2.1 General Geologic Information.

Material was obtained from the physiographic basin province known as the Salton Trough. This basin extends from south central California, in the United States, to northern Baja California, in México, and southwest into the Gulf of California, or the Sea of Cortez, as it is known in México. This basin has been a depository for clastic sediments that have been deposited since miocene time. (For a general survey, see Elders, 1979). These sediments were derived mainly from the Colorado River drainage of the Colorado Plateau Region. The cause of geothermal activity in the region is related to the fact that this basin marks the location of a major plate tectonic boundary between the North American and Pacific plates. For the work described here, core was obtained from the Cerro Prieto Field in México. Core obtained (described in more detail in the following subsection) can be described very generally as originating from a deltaic sedimentary sequence that has been altered by hydrothermal activity and also in some cases, by tectonic activity. Porosities of most of the sands are in the range from 10 to 40 percent, varying mostly with depth of burial, with the lower values being at the greater depths. These are typical values for normally consolidated sandstones. Permeabilities, on the other hand, are perhaps somewhat typically low for sands of their age and clay content. This is probably a result of hydrothermal

mechanisms, some of which tend to reduce permeability. (Large-scale fracture systems that would enhance flow in the geothermal systems are not observable in the laboratory). In general appearance, these rocks do not seem to be unusually susceptible to compaction, i.e., they are not weak or friable; however, nor are they unusually hard or strong. We hope that they are reasonably representative of many young, hydrothermal//geothermal sedimentary materials, in terms of their susceptibility to compaction, but there is certainly no large body of evidence to support this statement. Fluid samples or fluid chemistry information was also obtained. This was done to be able to maintain appropriate chemical equilibrium conditions during the testing of the rocks. The following subsections give detailed information on core obtained and on fluid properties associated with the reservoir.

### 2.2. Cerro Prieto.

Location of wells from which core was obtained in the Cerro Prieto geothermal field are shown in Figure 3.

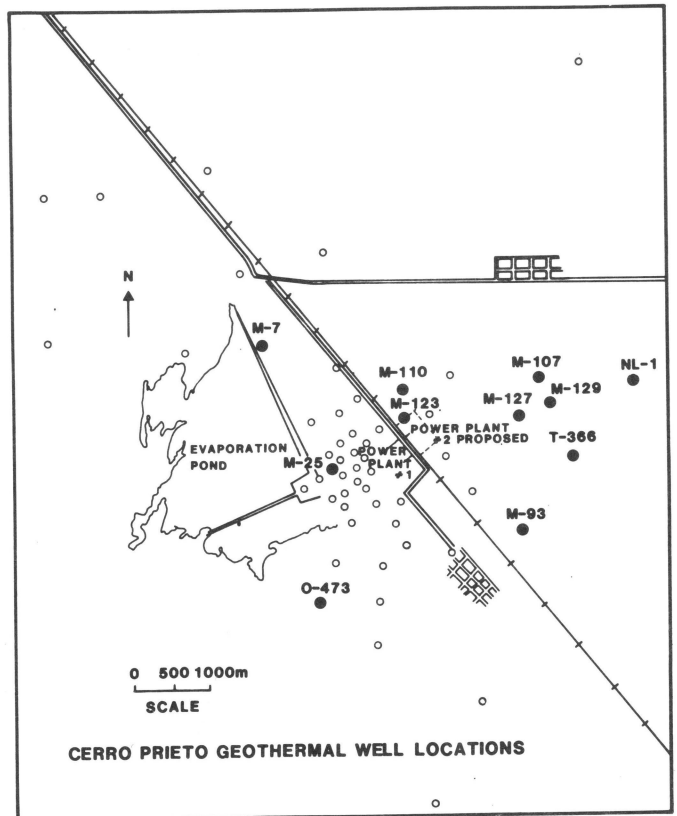


Figure 2. Map of Cerro Prieto geothermal well locations showing wells for which core was obtained for this program.

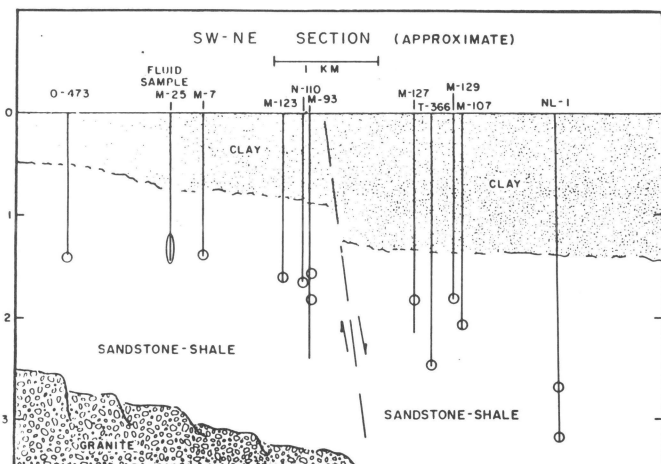


Figure 3. Schematic cross section of Cerro Prieto to geothermal field showing approximate depth from which core was obtained for this program.

A total of 40 feet of core from the Cerro Prieto field was kindly provided by Ing. Alfredo Mañón M., and his associates at the Comisión Federal de Electricidad. Specific well designations and depths are given in Table 1. Thin sections have been prepared from the core obtained and mineralogical results are given in Table 2. These rocks are, in general, fine to medium-grained sandstones with quartz contents in the range 60-70 percent. Porosities are in the range of 15-30 percent. They show many characteristics attributable to hydrothermal alteration. These include extensive quartz overgrowths, presence of epidote, alteration of plagioclase, and the occurrence of chlorite. Frequently, the quartz overgrowths have a sutured texture indicating that they are authigenic and not relics from a previous depositional cycle. Perhaps the best evidence of hydrothermal alteration is the abundant epidote that fills much of the pore space.

The calcite content of samples from each of the wells has been determined by a CO<sub>2</sub> evolution method. The calcite contents as determined are shown in Table 3. They fall into three categories. Wells, M-107, M-110, M-127, NL-1 and T-366 have essentially zero calcite. Wells M-7, and O-473 have approximately 1% calcite and wells M-93 and M-129 have approximately 6-8% calcite. Elders, et al (1978) have shown that the calcite content of Cerro Prieto rock correlates quite well with temperature boundaries in and near to the reservoir. Rocks with no calcite represent the hydrothermal reservoir itself in which calcite has been decomposed and replaced with minerals

Table 1  
Core Obtained from Cerro Prieto

Well	Depth (ft)
M-7	4600
M-93	5100, 5900, 6400, 7800
M-107	5300, 7000
M-110	5400
M-127	6100, 7100
M-129	5300, 5900
NL-1	9000, 10,500
O-473	4500
T-366	8200

Table 2  
Cerro Prieto Mineralogy

Classification	Well No.	Grains (% of Total)										Matrix (% of Total)			Porosity (%)	Roundness (Fowett, 1953)	Sorting	Quartz Overgrowths (Yes or No)	Mean Grain Dia. (mm)						
		Unaltered Qtz	Composite Qtz	Plagioclase	Albite	Microcline	Biotite	Muscovite	R.F. Chert	R.F. Shale	Epidote	Clay Minerals	Pyrite	Fe Oxide						Organic Matter	Calcite	Silica	Heatite		
Very Fine Grained Sandstone	T-366	66	-	-	5	2	T	-	-	-	12	-	5	-	1	-	-	5	-	20	Subangular to Subrounded	Mod Well	Yes	0.625	
Very Fine Grained Sandstone	O-473	72	-	T	2	1	5	-	T	-	3	5	-	-	1	-	-	8	-	23	Subangular to Subrounded	Mod Well to Poorly	Yes	0.1	
Medium Grained Sandstone	M-7	58	-	1	5	2	3	T	-	T	-	1	-	14	-	1	3	-	4	6	19	Rounded to Subrounded	Mod Well	Yes	0.35
Medium Grained Sandstone	M-93	58	-	-	3	2	-	2	-	-	-	T	-	10	-	4	-	-	15	3	39	Angular to Subangular	Mod Well	Yes	0.3
Coarse Grained Siltstone	M-107	51	-	-	2	-	-	T	-	-	-	15	-	20	-	3	-	-	5	5	25	Angular to Subangular	Mod Well	Yes	0.37
Fine Grained Sandstone	M-110	68	-	T	3	2	10	T	-	-	1	-	-	8	-	2	-	-	3	15	15	Subrounded	Mod Well	Yes	0.19
Fine Grained Sandstone	M-127	66	-	T	2	3	2	T	-	T	10	-	-	5	-	3	-	-	5	17	17	Angular to Subrounded	Poorly	Yes	0.15
Coarse Grained Carbonaceous Siltstone	M-129	56	-	-	2	T	-	-	T	-	4	-	-	12	-	5	-	-	15	2	17	Subangular to Subrounded	Mod Well	Yes	0.5
Fine Grained Sandstone	NL-1	49	-	T	7	4	7	-	-	T	6	-	-	15	-	-	-	-	6	18	18	Subangular to Rounded	Mod Well	Yes	0.13

representative of alteration such a silica and epidote. This corresponds to the zero calcite content group of five rocks. With temperature decrease (that is, moving upward in the reservoir, or moving downstream with respect to fluid flow

Table 3  
Cerro Prieto Core Calcite Contents

Well	Depth (m)	Porosity (%)	Calcite (%)
M-107	2115	25	0
M-110	1644	15	0
M-127	1871	17	0
NL-1	2735	18	0
T-366	2522	20	0
M-7	1410	19	1
O-473	1384	23	1
M-93	1566, 1804	39	6
M-129	1802	17	8

across the reservoir), one begins to encounter calcite in the rocks. This corresponds to the one percent calcite content rocks, which also have somewhat less silica and epidote as compared to the previous group. Calcite in this group could be either that which has not yet been dissolved or that which has been redeposited in the hydrothermal system as fluid has cooled. The third group of rocks, or those with 6-8% calcite in this case, are probably rocks located near the upper boundaries of the reservoir. To describe all groups in terms of temperature, the low calcite content rock may be expected to be from zones with temperatures well in excess of 250°C while the one percent or greater calcite content rock are expected to be from zones with temperature somewhat less than 250°C.

### 3. TESTING EQUIPMENT AND PROCEDURES

#### 3.1 General Information

Most of the equipment used for this program has been developed over a period of years at Terra Tek for purposes of testing at simulated in-situ conditions. In general, confining pressures of 60,000 psi, pore pressures of 30,000 psi, axial stresses of 150,000 psi (on two inch diameter specimens) and temperatures to 300°C, are handled routinely. In special cases, more extreme conditions can be created. Fluids can be light acids, brine, or alkalis, and in special cases, stronger acids or alkalis and heavier brines. Some new equipment was undertaken as part of this program to modify a test machine to be able to sustain constant test conditions for periods of weeks for the purpose of the creep measurements. In the following sections, test procedures and equipment will be described in the major categories of preliminary sample handling, basic testing, creep testing, fluid chemistry, and microstructural analysis.

#### 3.2 Preliminary Sample Handling.

The first step in sample handling was the acquisition of core. At Cerro Prieto, core was selected from shelves at the storage warehouse at the geothermal field. With little exception, the core available had been stored dry on the shelf for a period of months to years. It was boxed and shipped to Terra Tek. Upon receipt at Terra Tek, it was logged in and saved for testing. There were, unknown possibilities of sample handling disturbance and, due to drying, clay alteration in the Cerro Prieto material. However, the relatively small amount of clays in these materials and the stability of the products of hydrothermal alteration at room temperature lead us

to feel confident that the Cerro Prieto material was received in a testable condition. As a check, some comparison tests for Cerro Prieto material were made on a small quantity of core that had been preserved, and re-aerated core that had been previously dried. No discernible differences aside from normal random variation were seen in the mechanical properties results from these tests.

The test program for this project was designed to emphasize tests on sands from production zones, as these would see the greatest pore pressure decrease and probably have the greatest tendency to compact. To start, small pieces of material were chipped or cut off from cores near to the locations where test samples were to be cut. With these pieces a wet density, a dry density, and a grain density were determined by immersion and gas pycnometer techniques. From these values, a porosity for each specimen was determined. Results are given later in the section on test results. Also, from similar pieces, samples were prepared for thin section and scanning electron microscope analysis. The thin section preparations were either conventional impregnations, blue stain impregnations for porosity determinations, or red stain impregnations for calcite determinations. The SEM specimens were chipped to provide a fresh tensile surface for viewing.

Samples for in-situ condition testing were prepared in the form of right cylinders. For basic testings, samples were generally 1-1/2 inches in diameter by 3 inches in length. For creep testing and permeability testings, samples were generally two inches in diameter by four inches in length. These samples were cut in a water spray and then the ends were ground to provide flat and parallel surfaces within  $\pm 0.005$  inch. Test specimen were then placed between two cylindrical stainless steel end caps as shown in Figure 4. The end caps had provision for pore fluid connection to the test samples. The samples were encased in a tube of heat-shrinkable teflon and ends were sealed with stainless steel lock wire. These samples were then placed into the appropriate machine for testing. Detail of procedures associated with fluid saturation, pore pressure control, and other pressure and temperature controls will be described below in the individual section for each test procedure.

#### 3.3 Basic Testing.

The purpose of this part of the testing program was to fully characterize the materials in terms of basic properties such as compressibility at reservoir

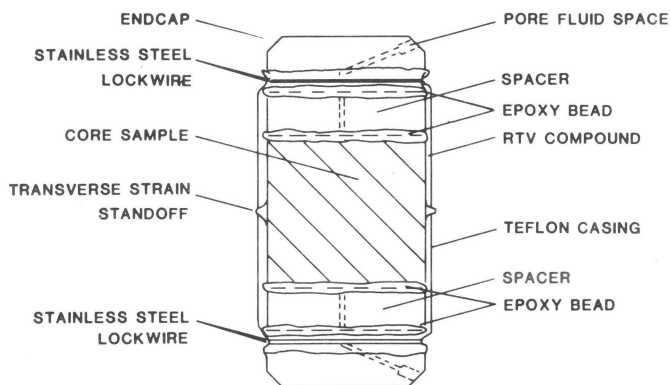


Figure 4. Schematic diagram of assembled test specimen showing sample, endcaps, jacket, and pore fluid connections.

conditions and also to determine if different types of testings such as confining pressure increase, pore pressure reduction, and one dimensional (uniaxial) strain, significantly altered sample behavior.

In all tests, the prepared specimen, including rock, end caps, and jacket, was placed in the test machine. Pore pressure lines were connected and the machine was sealed and filled with a light mineral oil confining fluid. In most tests, the sample was backfilled with a saturating fluid. Usually, this was a simulant of reservoirs brine. Backfill of fluid was achieved by first evacuating the pore pressure system and then opening the system with a valve let brine in without air. Fluid was thus allowed to flow back into the core and equilibrate to fill the pore space. This has been to be a consistent and adequate way of achieving at least 95 percent saturation in a material that has a permeability of more than a few millidarcies.

One prepared in this manner, the specimen was tested. The test system was capable of applying and measuring confining pressure, pore pressure, axial stress, and temperature. Strains were also measured. In this system, both axial and transverse strains were measured by a cantilever system. This system was calibrated at frequent intervals and was accurate to  $\pm 0.001$  inch. In this case, this accuracy corresponds to a few hundredths of one percent strain or a volume strain of about one-tenth of one percent. Load, when applied to the specimens to create axial stress, was via a piston directly contacting the upper end cap. Load was measured by a strain-gaged load cell which was also frequently calibrated. The specific types of basic tests run were:

### 3.3.1 Drained and Undrained Hydrostats.

Initial tests were run at room temperature. Specimens were prepared, saturated as described above, and then confining pressure was increased to approximate reservoir conditions. In some tests, during confining pressure increase, fluid was allowed to drain from the specimen at a small constant pore pressure. This test, termed a "drained test", was a measure of the rock skeleton compressibility or reservoir compressibility. In other tests, the pore pressure systems was locked off and the pore pressure was allowed to increase as confining pressure was increased. This test, termed and "undrained test", was more nearly a test of rock grain and fluid compressibility. Both of these test types were used to determine the most appropriate concept of effective stress in these materials.

### 3.3.2 Room Temperature and High Temperature Drained Hydrostats.

Following sample preparation and saturation as described above, drained hydrostats were run on similar materials at both room and elevated temperatures. The purpose of these tests was to determine the effect of temperature variation on the response of these specimens. It would thus be used to determine the importance of testing at elevated temperatures in the remainder of the program.

### 3.3.3 Cycling.

Some tests were conducted with multiple cycles of pressure increase and decrease. This was to determine the amount of cycling-caused hysteresis and its effect on overall behavior. This could be an important factor for planning of reservoir production that involves alternate cycles of discharge and recharge.

### 3.3.4 Pore Pressure Reduction.

During reservoir production, compaction will be triggered by pore pressure reduction and the resulting increase of effective stress. During this program, this effect was studied by bringing the rock to approximate reservoir conditions and then reducing pore pressure while measuring specimen compaction. Tests described previously were hydrostatic. That is, they were without additional axial load on the specimen. Pore pressure reduction tests, instead, were done at appropriate "triaxial" conditions of axial load and confining pressure to approximate actual stress conditions in the reservoirs.

### 3.3.5 Uniaxial Strain.

For some compaction and subsidence models, it is useful to measure, instead of hydrostatic or triaxial compaction, a compaction that occurs for uniaxial strain, that is, with no change in the transverse dimensions of the specimen. Specimens for these test were brought to reservoir conditions, and then pore pressure was reduced. However, instead of keeping axial and confining stresses constant, while reducing pore pressure as in the triaxial test, the transverse strain was held constant. To do this, it was necessary to continually adjust confining pressure.

### 3.3.6 Ultrasonic Velocities.

In combination with many of the above tests, ultrasonic compressional (P) and shear (S) wave velocities through the specimens were measured as effective stress was varied. This was done for field sonic log correlation and to determine if field-determined sonic velocities could be used as a measure of reservoir compaction.

### 3.4 Creep Testing.

Each test in the basic testings sequence was accomplished in less than one hour of time (not including set-up). Because of the long-term effects of elevated pressure and temperature, compaction could have significant time dependence that would not be recognized in such a short-term test. For this reason, it was decided to do a number of additional test at reservoir conditions with pore pressure reduction for extended periods of time, up to several weeks. With long-term equilibrium now important, care was taken during these tests to control and understand the fluid chemistry phenomena that were occurring. As will be seen later, certain changes in fluid chemistry during creep tests are possibly linked to evidence or mechanisms of mechanical alteration. Also during this phase of work, some permeabilities at reservoir condition were measured.

Confining pressure, load, and temperature were monitored in the creep system. Additionally, measurements included transverse strain, axial strain, and in some cases, pore volume change. The axial strain measurements were achieved by direct measurement of sample length using two LVDTs (Linear Variable Differential Transformers). These were more accurate and stable than the cantilever system used for basic testing. Sample length could be resolved to approximately  $\pm 0.0005$  inches. Also, on shortterm tests, transverse strain

measurements were achieved by use of strain-gaged cantilevers as described previously. The resolution of this system was approximately  $\pm 0.001$  inch. Volume strain of the entire specimen could be resolved to better than 0.1 percent. Additionally, pore volume change could be measured by an LVDT system mounted on the pore pressure accumulator. A volume change of  $\pm 0.05$  cm<sup>3</sup> could be resolved. For flow experiments, the differential pressure transducer allowed  $\pm 3$  psi of differential pressure (across the specimen) to be resolved.

The creep testing procedure used was as follow: Following acquisition, characterization, and preparation, the sample was placed into the test machine. It was then saturated using a backfill procedure as described in the basic testing section. A small amount of confining pressure (usually 100 psi or less) was used at this point to assure intimate contact of jacket and specimen. Saturation was then guaranteed by flowing pore fluid through the specimen. In some cases, permeabilities were measured while fluid flowed through the specimen at these conditions.

Most of the specimen tested had residues of drilling muds and brine solids left in the specimen. To insure that these were all removed from creep test specimen, fluid was flushed through the sample and chemically analyzed at the output until composition of output fluid did not differ significantly from input fluid. It was thus determined that equilibrium had been achieved at low temperature. The sample was then raised to in-situ stress-simulating conditions of confining pressure, pore pressure, and axial load. Care was taken during this loading phase to no exceed the in-situ effective stress. This was achieved by increasing all quantities simultaneously. Such that effective stress was monotonically increased to reservoir conditions. This cautious treatment was important, as it prevented pre-cycling of the sample in an unrealistic manner. Once at pressure, the fluid composition was adjusted to the proper chemistry by alteration of its CO<sub>2</sub> content, and the sample was again flushed. In some cases, permeability was again measured. At this point, the sample was slowly and carefully heated to reservoir temperature. Pressures were controlled carefully during this heating to account for thermal expansion effects. More fluid was then flushed through the specimen and in some cases, permeability was measured. Then, the samples was allowed to stabilize until it showed no strain fluctuations as caused by thermal equilibration of the machine. Then, creep was initiated by quickly lowering

the pore pressure by approximately 1000 psi, therefore simultaneously increasing the mean effective stress by approximately the same amount. During this stress increase, a short-term or "elastic" compressibility was determined for comparison with previous results obtained during basic testing. Shortly after creep initiation, another permeability was sometimes measured.

Care was taken to maintain constant stresses and temperature for the duration of the creep period. At the end of the creep period, in many cases, another permeability was measured in order to correlate permeability reduction with creep compaction. Finally, pore pressure was raised to its initial value and a final compressibility, and in some cases, permeability, was determined. A fluid sample was also obtained for chemical analysis. Then the sample was cooled, removed from the machine, and its jacket removed. Small samples were taken for post-test thin section, and scanning electron microscope analyses.

### 3.5 Fluid Chemistry.

Testing of fluid-bearing reservoir rock, whether it be for geothermal, oil and gas, or water reservoirs, should be done with fluids that are compatible with rock structure and consistent with in-situ chemistries. The classic example of the validity of this procedural recommendation is the necessity to test a rock containing swelling clays with fluids that are in ionic equilibrium with the clays. Otherwise, non-equilibrium fluids would cause significant permeability and porosity alterations. Less is known about non-equilibrium fluid effects for the case of testing of geothermal reservoir rocks, however, it is certainly true that during long-term creep testing, fluid chemistry and rock-fluid equilibria can potentially affect the chemical and mechanical make-up of these rocks. Furthermore, with control and measurement of fluid chemistry, chemical information can be used to assist in determining the mechanism of creep.

The objectives of fluid chemistry control and analysis for this program were to minimize chemically-induced rock response during testing procedures and to determine chemical indicators of mechanical creep-compaction mechanisms. To minimize undesired chemical reactions it was necessary to use as pore fluid either an actual geothermal brine or a synthetic brine with the correct composition. Both brine types have been used during this testing program.

To insure that chemical equilibrium

was being approximated during testing in the laboratory, it was necessary to periodically sample the pore fluid and analyze it for major constituents. Analyses were performed both in Terra Tek's chemistry laboratory and in the geochemical laboratory at the University of Utah. However, most of the fluid used in the Cerro Prieto tests originated from brine sampled at the geothermal field. The brine was collected from well M-129 downstream of the separator and consequently, it was concentrated with respect to dissolved solids due to the loss of 30-40 percent by weight of steam. In the field, the sampled fluid was acidified with nitric acid to a pH of about two, to minimize precipitation of silica and calcium carbonate during storage. Analyses of this fluid have shown that the acidified brine can be stored for months with very little alteration.

The field sampling and fluid treatment sequence is shown in Figure 5. Immediately prior to use in the laboratory (within 24 hours), two to four liters of stabilized brine were diluted with deionized water and pH-adjusted with sodium hydroxide to approximate downhole conditions. The values for the major constituent, for the concentrated, adjusted and estimated in-situ brines are given in Table 4. Although the concentrations in the fluid used in testing do not correspond exactly to the estimated downhole values, they are, with the exception of calcium bicarbonate, well within the range of values observed at the Cerro Prieto field. The low concentration of calcium carbonate during flashing and the liberation of carbon dioxide gas due to acidification. Once the fluid was prepared for the test, it was introduced to the pore pressure system and pressurized in an accumulator.

For creep tests, considerable flushing prior to actual testing was done, as described above in the creep testing section. Analyses have shown that flushing primarily removed salts and drilling mud residues left by coring operation. After initial flushing, when downstream chemistry was acceptable, the specimen was brought to in-situ conditions and allowed to stabilize. The pore fluid was again sampled and compared to the input fluid. If the chemistry was not acceptable, additional flushing was performed at in-situ conditions, otherwise, the test proceeded. At the conclusion of the test, a volume of pore fluid equal to approximately one-half to three-fourths of a pore volume (20-30 cubic centimeters) was sampled and analyzed for its constituents. These values were then compared to those for the



**CERRO PRIETO FIELD SAMPLING &  
LABORATORY CHEMISTRY CYCLE**

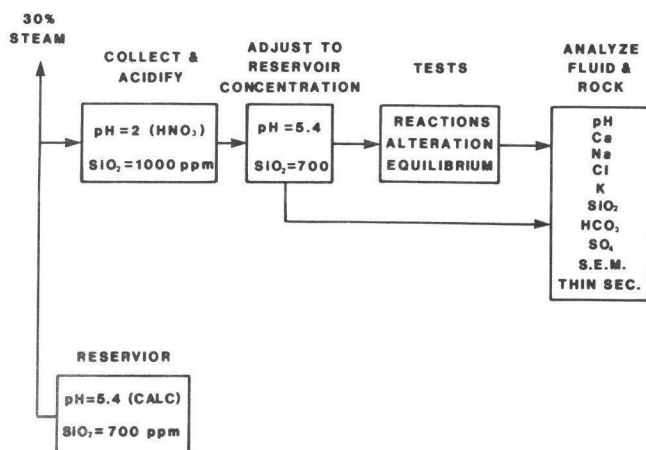


Figure 5. Flow chart of cycle through which fluid from the Cerro Prieto reservoir was taken between sampling at the wellhead and final analysis after testing.

Table 4

Cerro Prieto Brine Composition

Constituent	As Received <sup>1</sup>	In-Situ <sup>2</sup>	Test Cell
pH	1 - 2	5.4	5 - 6
Ca	430 ppm	370	270
Na	6,550	5,100	6,000
Cl	16,700	9,700	13,000
K	1,550	1,100	1,200
SiO <sub>2</sub>	990	540	650
HCO <sub>3</sub>	0	1,800 (Aq. CO <sub>2</sub> )	0
SO <sub>4</sub>	0	20	0
TDS	28,220	17,000 - 20,000	20,000

<sup>1</sup>Brine used in testing is actually sampled from The Cerro Prieto Field. As received fluid is sampled after the separator, and thus is concentrated due to flashing off of 30 - 40% of liquid.

<sup>2</sup>Source: Reed, 1976. Average of 12 wells.

original input fluid to give insight to the degree of equilibrium achieved, completeness of flushing, and alteration to the specimen.

### 3.6 Microstructural Analyses.

Three procedures were used for microstructural analyses: thin section petrographic analysis, x-ray diffraction and scanning electron microscope analysis. In most cases, samples were studied with one or more procedures both before and after creep testing. The main objective of post-test analysis was to identify microstructural mechanisms

of creep compaction. Thin sections were prepared and studies of basic mineralogy of the specimen were done at Terra Tek. These were especially valuable for study of the pre-test materials. For post test studies, although thin sections were useful, it was found that the scanning electron microscope was much more information. X-ray diffraction was done at the University of Utah on both pre- and post-test specimens to study clay alterations. The x-ray diffraction was carried out with Cu K- alpha radiation at 40 KV accelerating potential and 20 MA current. In general, three sets of scans were done for each sample, the first on an air-dried specimen, the second on a specimen exposed to ethylene/glycol vapor for several hours, which caused expansion of swelling clays, and the third on a sample heated to 550°C, which destroyed any kaolinite present. These methods allowed separation of clay types. The scanning electron microscope analysis was carried out at the University of Utah by Terra Tek personnel. Samples were prepared by tensile fracturing and mounted on a sample holder followed by ultrasonic cleaning. In addition, the SEM used had a computerized energy dispersive analysis by X-ray (EDAX) system, which allowed a quick determination elemental composition along with each SEM frame. The SEM work was used to characterize porosity and pore throat structures, to identify dissolution of minerals during tests and to look for possible growth of authigenic phases caused by testing.

## 4. BASIC TESTING RESULTS.

In this section results will be presented in the form of graphs of mean stress versus volume strain, where mean stress is defined as the average of the three principal stresses. In the case of the hydrostatic test, the mean stress is exactly equal to the confining pressure. In the case of any test where additional axial stress has been applied (triaxial, uniaxial), the mean stress is the confining pressure plus one-third of the additional axial stress applied. In tests where pore pressure has been applied and measured, stress values will be presented in terms of mean effective stress. In this case, we will use the Terzaghi effective stress, defined as the total mean effective stress (as given above) less the pore pressure. Graphs of mean effective stress versus volume strain may easily be interpreted in terms of specimen compressibility. This will be the best way of comparing data from test to test.

### 4.2.1 Drained Hydrostats

Drained hydrostats are a basic

measure of skeletal deformation. These tests were done on saturated specimens that were allowed to drain during the test at low pore volume. Typical results of basic testings are shown in Figures 6-8. A drained hydrostat at room temperature on material from well M-123 is shown Figure 6. This result is typical of porous sandstone. Compressibility is about  $1 \times 10^{-6}$   $\text{psi}^{-1}$  at reservoir pressure and some hysteresis was evident. Figure 7 shows hydrostatic compression of material from well T-366 from a depth of greater than 8,200 feet. Note, however that porosity was greater than for the previous well, and that these tests were at elevated temperature. Despite the differences in depth and temperature, the compressibility at reservoir conditions was approximately the same for this test as for that of the previous well. Also, repeatability was good. Figure 8 shows another drained hydrostat at elevated temperatures on material from the same well, T-366. However, this material was from a slightly different location and had considerably less porosity. Note, however, that compressibility is comparable to the previous test. This could indicate that the material causing the lowering of porosity is a softer material that does not contribute to strengthening or stiffening of the structure.

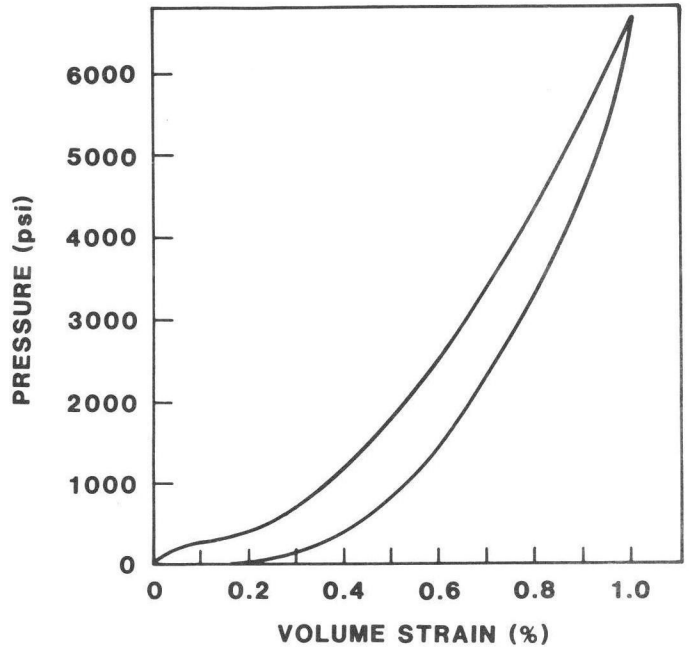


Figure 7. Drained hydrostat on material from Cerro Prieto well T-366, depth 8,269', porosity 19.8%, test temperature 90°C, compressibility at 5000 psi  $1.1 \times 10^{-6}$   $\text{psi}^{-1}$

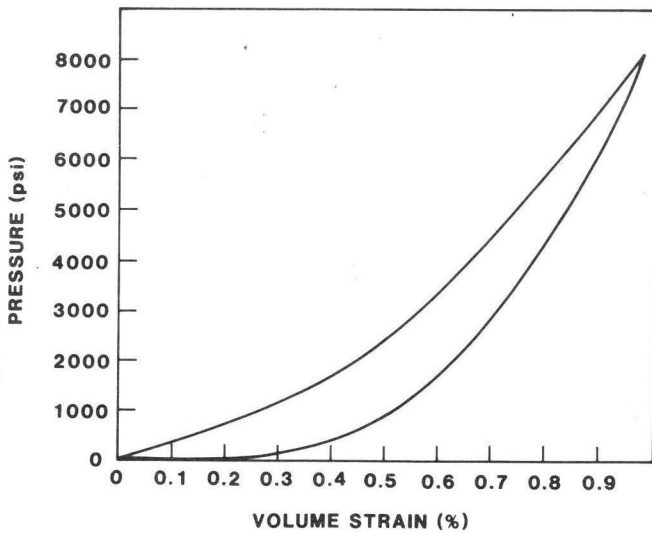


Figure 6. Drained hydrostat on material from Cerro Prieto well M-123, depth 5,200', porosity 14.9%, test temperature 25°C, compressibility at 3000 psi  $1.1 \times 10^{-6}$   $\text{psi}^{-1}$

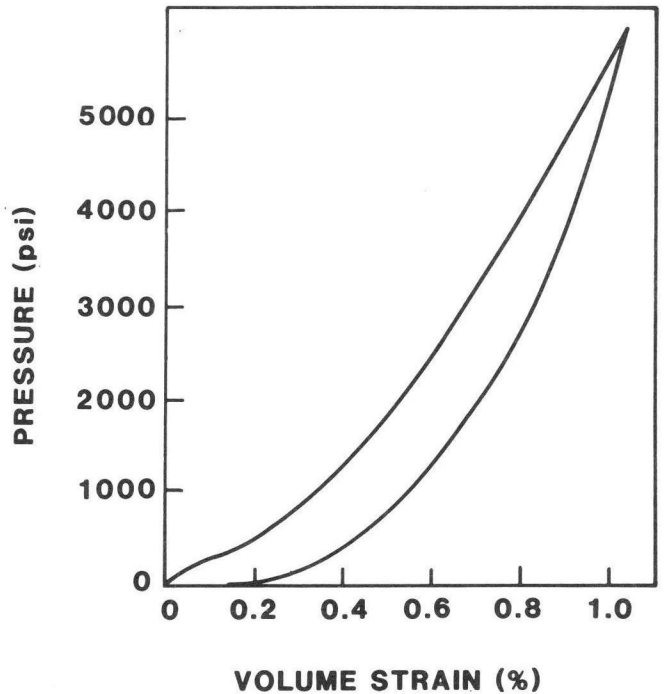


Figure 8. Drained hydrostat on material from Cerro Prieto well T-366, depth 8,269', porosity 13.7%, test temperature 90°C, compressibility at 5000 psi  $1.2 \times 10^{-6}$   $\text{psi}^{-1}$

#### 4.2 Pore Pressure Reduction

To truly simulate the field conditions, it was necessary to test at elevated temperature and at the stresses

actually seen in the reservoir. The tests described in this section were carried out at elevated temperatures and at total overburden axial stresses corresponding to those existing in the reservoir. However, since lateral tectonic stresses vary and are mostly unknown in these regions, various confining pressures were used on material from each depth to span the range of possible ratios of lateral to vertical in-situ stress. These conditions are given in Table 5. The tests were conducted by first carefully bringing the

Table 5

Initial Conditions, Cerro Prieto  
Pore Pressure Reduction Tests

Well	Depth (ft)	Stress or Pressure (psi)			Temperature (°C)
		Confining	Pore	Axial	
M-107	7070	2300	3100	4630	150
		4630	3100	2300	
		6940	3100	0	
M-127	7140	2380	3200	4760	150
		4760	3200	2380	
		7140	3200	0	
T-366	8010	2670	3600	5340	150
		5340	3600	2670	
		8015	3600	0	

rock to the approximated reservoir conditions, taking care to not exceed the mean effective stress at reservoir conditions prior to the pore pressure cycling part of the test. Then, pore pressure was reduced by 1000 psi to simulate well production. The pore pressure was cycled three times to investigate hysteresis effects that would be caused by alternate pressure reduction and recharge. In some cases, conditions were held constant for periods of up to about 30 minutes to investigate the primary phase of creep behavior for later use in creep testing. Typical results, in terms of mean effective stress versus volume strain, are shown in Figure 9-12. Material was selected from three wells for this study. They were well M-107 with material from 7,067 feet, well M-127 with material from 7,136 feet, and well T-366 with material from 8,010 feet. The highest shear stress ratio generally caused failure of test specimens. Therefore, only typical low and intermediate shear stress ratio results are shown in the figures. Compressibilities in these three wells were quite comparable, and all in the range  $0.6$  to  $0.9 \times 10^{-6}$   $\text{psi}^{-1}$ . There was no significant trend to increased plastic behavior as shearing stresses were increased, nor was there any significant hysteresis caused by cycling. These observations, coupled with the tendency for failure at the higher shear stress values, indicated

that these sandstones were essentially elastic-brittle in nature.

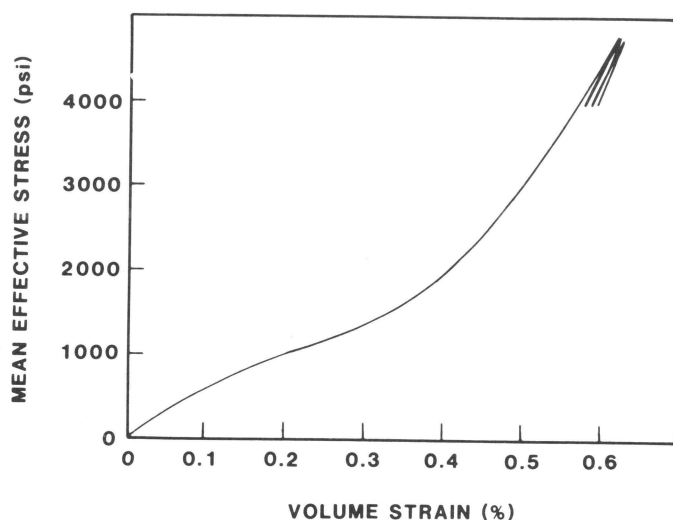


Figure 9. Pore pressure cycling test on material from Cerro Prieto well M-107, depth 6,936', porosity 18.9%, no shear stress, test temperature 150°C. Compressibility  $0.6 \times 10^{-6}$   $\text{psi}^{-1}$  for effective stress increase and  $0.5 \times 10^{-6}$   $\text{psi}^{-1}$  for effective stress decrease.

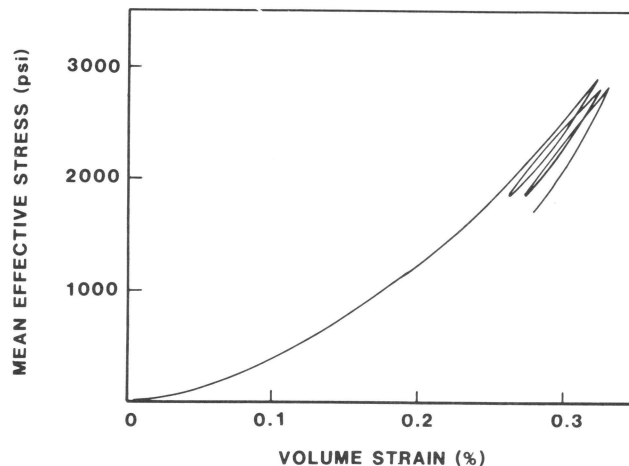


Figure 10. Pore pressure cycling test on material from Cerro Prieto well M-107, depth 6,936', porosity 18.6%, intermediate shear stress, test temperature 150°C. Compressibility  $0.7 \times 10^{-6}$   $\text{psi}^{-1}$  for effective stress increase and  $0.5 \times 10^{-6}$   $\text{psi}^{-1}$  for effective stress decrease.

#### 4.3 Confining Pressure Cycling and Uniaxial Compaction.

The remaining basic tests were a combination of two types of testings. For this testing, specimen were brought to conditions of elevated pressure and temperature as before, but then, instead of reducing pore pressure, confining pressures was increased by 1000 psi and cycled. This procedure served the

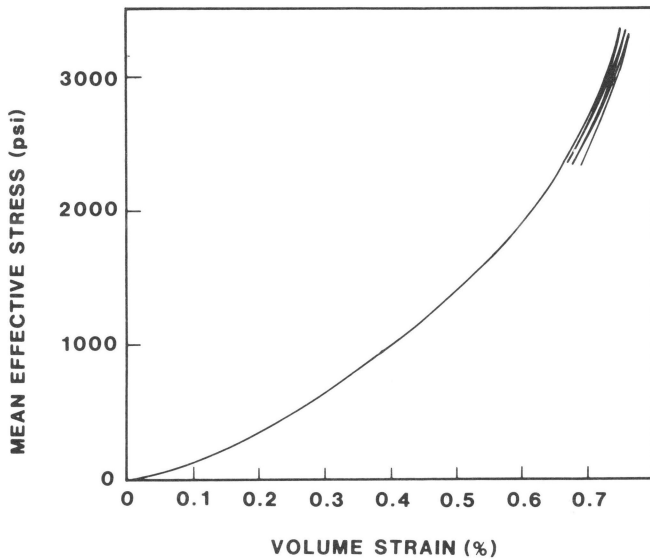


Figure 11. Pore pressure cycling test on material from Cerro Prieto well M-127, depth 7,136', porosity 19.4%, intermediate shear stress, test temperature 150°C. Compressibility  $0.9 \times 10^{-6} \text{ psi}^{-1}$  for effective stress increase and  $0.7 \times 10^{-6} \text{ psi}^{-1}$  for effective stress decrease.

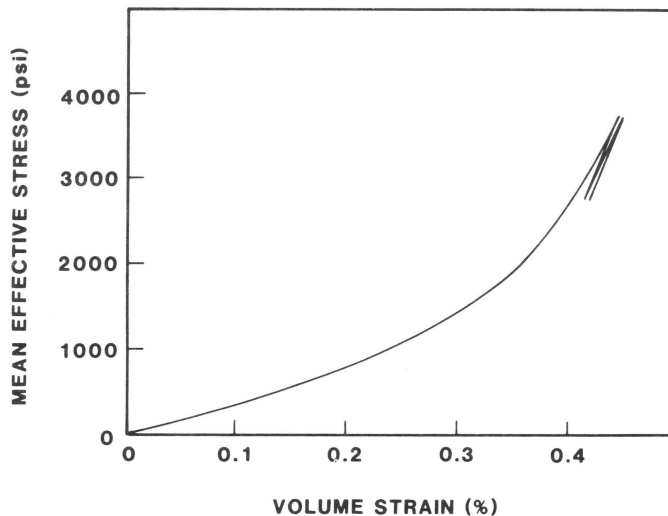


Figure 12. Pore pressure cycling test on material from Cerro Prieto well T-366, depth 8,010', porosity 19.3%, intermediate shear stress, test temperature 150°C. Compressibility  $0.5 \times 10^{-6} \text{ psi}^{-1}$  for effective stress increase and  $0.3 \times 10^{-6} \text{ psi}^{-1}$  for effective stress decrease.

maintain zero incremental transverse strain during the pore pressure reduction cycle. This was done to obtain a compressibility coefficient for uniaxial compaction. Typical results of these tests are given in figures 13 and 14. Stress conditions to start these tests were the same as for the intermediate shear stress tests of the previous section. For confining pressure cycling, results were similar to the previous results. There was possibly a small trend to larger compressibility, which would be consistent with a non-zero grain compressibility which altered the Terzaghi effective stress. Uniaxial compacting results indicated a slight tendency to greater effective compressibility; however the change was not marked and it was consistent with the relatively elastic short-term response of Cerro Prieto material.

#### 4.4. Ultrasonic Velocities.

Ultrasonic velocities measurements were performed on Cerro Prieto material from the three wells as described above. These were done both at reservoir conditions and for reduced pore pressure. The purpose of these measurements was to look for correlations with other test results, and, in particular to determine the extent that ultrasonic velocities might be sensitive indicators of compaction phenomena. If this were true, then downhole sonic measurements could be used as compaction indicators in the field.

Ultrasonic velocity results are shown in Table 6, where P and S wave velocities at reservoir conditions and at reduced pore pressure (by 1000 psi) are shown. There was a change in average velocity corresponding to compaction of one to two percent. This change, however, was probably not significant enough to be readily discernible downhole, considering the perturbing influences of other mechanism, such as noise caused by fluid flow, tectonics, thermal fluctuation, etc. Nevertheless, in the laboratory, the change was consistent and easily measurable.

#### 5. CREEP TESTING RESULTS.

Basic testing, as described in the previous section, succeeded in determining the short-term compressional response properties of Cerro Prieto cores. The loading duration of these short-term compressional response properties of Cerro Prieto cores. The loading duration of these short-term test was, in most cases, less than one hour. Some evidence of time-dependent inelastic

purpose of checking the trends of previous data and also of studying the accuracy of the Terzaghi effective law as applied to this material. Following the confining pressure cycling, a final effective stress increase was produced by reduction of pore pressure as in the previous section. However, in this case, confining pressure was adjusted to

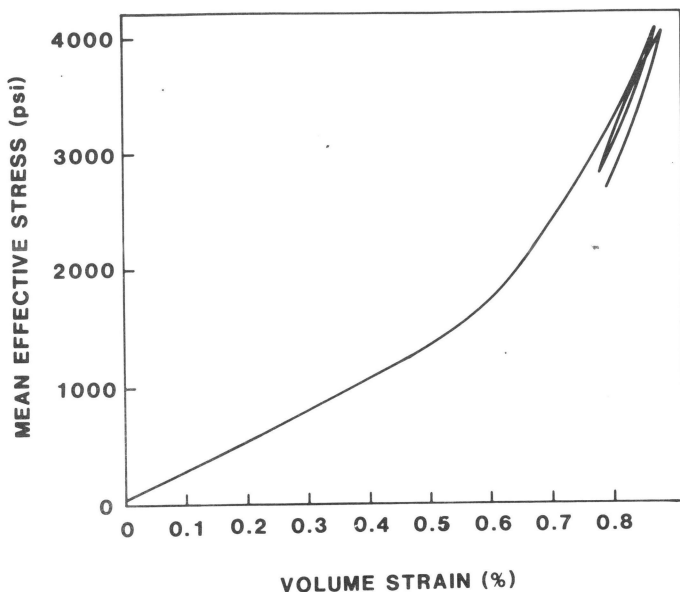


Figure 13. Confining pressure cycling test on Cerro Prieto material from well M-127, depth 7,136', porosity 20.4%, test temperature 150°C, intermediate shear stress. Compressibility  $1.0 \times 10^{-6}$  psi<sup>-1</sup> for effective stress increase and  $0.7 \times 10^{-6}$  psi<sup>-1</sup> for effective stress decrease.

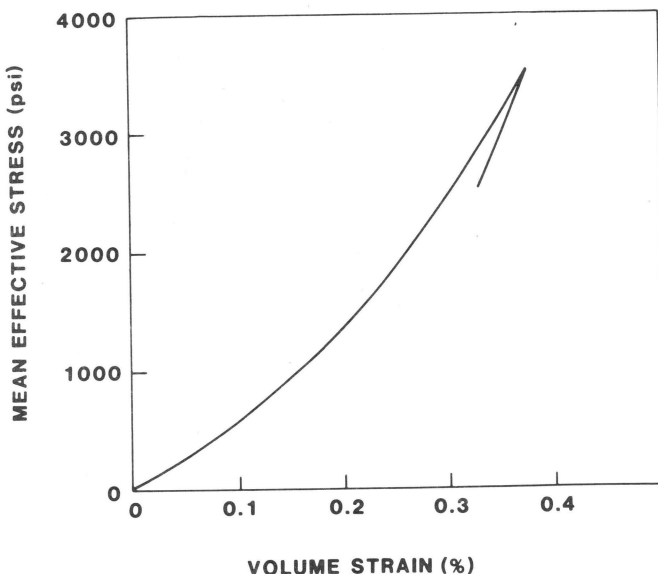


Figure 14. Uniaxial compaction test on material from Cerro Prieto well M-127, depth 7,136', porosity 21.6%, test temperature 150°C, compressibility  $0.7 \times 10^{-6}$  psi<sup>-1</sup>.

response was observed. This suggested that they may also exhibit long-term creep compaction if large effective stresses were maintained for long periods of time. The purpose of creep testing, therefore, was to determine the extent that compaction is time-dependent, thus making long term effective compressibilities larger than those measured in short-term tests. Additionally, since reservoir permeabilities may be affected by long-term compaction, several creep tests also included measurements of permeability.

Table 6

Ultrasonic Velocities  
Cerro Prieto (km/s)

	M-107		M-127		T-366		Average	
	V <sub>p</sub>	V <sub>s</sub>	V <sub>p</sub>	V <sub>s</sub>	V <sub>p</sub>	V <sub>s</sub>	V <sub>p</sub>	V <sub>s</sub>
Reservoir Conditions	4.01	2.52	3.82	1.96	4.03	2.61	3.95	2.36
Reduced P <sub>p</sub>	4.06	2.57	3.90	2.01	4.05	2.66	4.00	2.41
Change (%)	+1.1	+2.0	+2.1	+2.5	+0.4	+1.7	+1.3	+2.2

Tests were generally run at temperature in the range 250°C to 300°C. Generally, total overburden stress was set equal to one psi per foot of burial, pore pressure was set by assuming a normal hydrostatic gradient, and confining pressure was set so that the ratio of effective overburden to effective lateral stress was approximately three to two. In most cases, only axial strains were measured during the creep tests. (Early creep testing indicated that the lateral strain system, which consisted of strain-gaged cantilevers, was subject in some cases to more long-term drift than the axial strain system, which consisted of LVDT's. Therefore, to obtain maximum resolution for purposes of creep compaction measurement, only the higher resolution axial strain LVDT measurements were used). Resolution of creep strain was about  $1 \times 10^{-4}$ /day or  $1 \times 10^{-9}$ /sec. Creep results are presented here as curves of volume strain versus time. For constant grain volume and small strains, the volume strain versus time curves may be treated also as porosity change versus time curves.

5.1 Initial Creep Tests, Cerro Prieto.

Initially, nine tests were conducted on material from nine different wells at Cerro Prieto. Creep duration ranged from 120 minutes to 550 minutes and permeabilities were measured several times during each test. The description of results will be separated into two subsections; the first describing volume strain results, and the second permeability results.

### 5.1.1 Volume Strain Results.

Typical volume strain results are given in Figures 15-17. Generally, as material becomes coarser-grained or contains more silt, creep becomes more noticeable; however, results are highly variable. Creep amounts in these materials vary from little or none in rocks from Wells M-127, M-110, O-473 and NL-1. Note that these materials are all relatively fine-grained and that they tend to contain little or no calcite (see Table 2). Higher creep rates are observable in samples from wells M-7, M-107 and M-129. These all tend to be coarser-grainer materials. Finally, and extremely high creep rate is observed in the sample from well M-93. This sample was very friable, had high porosity, and was clearly different from other materials

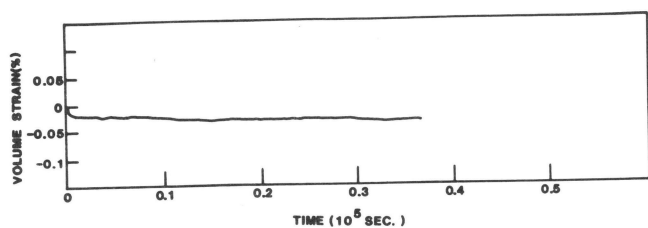


Figure 15. Creep compaction test on material from Cerro Prieto well 0473, creep rate is approximately  $1.7 \times 10^{-9} \text{ sec}^{-1}$ .

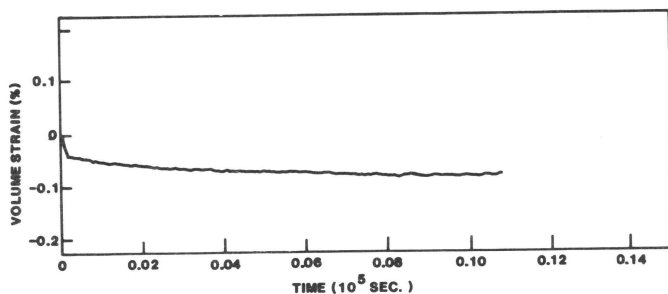


Figure 16. Creep compaction test on material from Cerro Prieto well M-129, creep rate is approximately  $13.3 \times 10^{-9} \text{ sec}^{-1}$

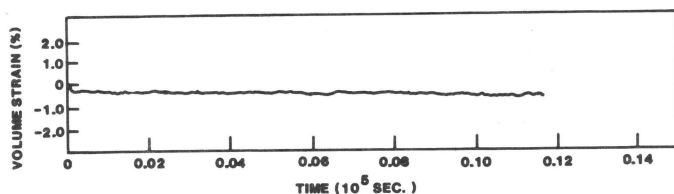


Figure 17. Creep compaction test on material from Cerro Prieto well M-93, creep rate is approximately  $87.0 \times 10^{-9} \text{ sec}^{-1}$

longerterm Cerro Prieto tests, as shown in Figures 26-28, the average creep rate is somewhat less at about  $2 \times 10^{-9} \text{ /sec}$ .

### 5.1.2 Permeability Results.

Permeability results are shown in Table 7. Results are quite variable. During permeability testings, it became evident that fluid chemistry was playing

Table 7  
Permeabilities, Cerro Prieto (md)  
(All at In-Situ Pressures)

	Room Temp.	Elev. Temp.	Pp Red.	Post Creep	Pp Inc.	Comments
CP1 M127	1.8	1.7	1.3	--	--	Low Calcite
CP2 M110	1.0	0.7	0.8	--	--	Low Calcite
CP3 0473	3.0	--	0.14	0.07	0.13	
CP4 T366	--	0.70	0.76	0.37	0.40	Low Calcite
CP5 M7	--	--	6.0	3.0	--	
CP6 M107	0.5	0.22	0.21	0.11	0.20	Low Calcite
CP7 M129	--	--	0.25	0.23	--	
CP8 NL1	3.0	1.2	1.2	0.9	0.9	Low Calcite
CP9 M93	14.5	7.3	--	5.8	--	
Avg.	4.0	Temp Chg. -40% ± 23%	Pp Chg -1% ± 15%	Creep Chg -39% ± 18%	Pp Inc. +44% ± 46%	

an important role in the behavior of this material. As will be seen in the fluid chemistry results section, this was particularly noticeable in the case of rocks that contained relatively large amounts of calcite. The carbonate equilibrium seemed to control the amount of fines that could be released from the rock. As a result, there were extreme problems with plugging of high carbonate rock in permeability tests. Results are averaged in the last line of Table 7. They are shown in term of initial average values and changes from those average as percentages from the previous value. The average permeability measured is about 4 millidarcies. With increased temperature, there is a reduction of permeability by about 40 percent. One standard deviation of this value is about 23 percent, so this reduction is moderately significant. With pore pressure reduction to increase effective stress, there is no significant change in permeability. With creep, there is a reduction of approximately  $39 \pm 18$  percent, which is significant. With final pore pressure increase, there is considerable scatter in results, but with

obtained from wells at Cerro Prieto. In fact, with its high initial creep rate, it perhaps behaved more as a soil than as a rock. When all results except well M-93 are averaged, the observed creep rate is  $7.2 \times 10^{-9} \text{ /sec}$ . If one looks only at the

statistical significance, there is no change in permeability from post-creep values.

To summarize, we have seen that in rocks from Cerro Prieto, permeability is reduced by increase of temperature to near in-situ conditions by creep, but it is not reduced in conjunction with the instantaneous reducing of pore pressure. This is interesting, because for the duration of time of these creep tests, the total creep strains were not larger than the instantaneous strains caused by pore pressure reduction. There are two possible explanations for this. One is that the permeability reductions associated with creep are somewhat anomalous, having been caused by particulate plugging as a result of chemical non-equilibrium effects. However, indications of non-equilibrium were small for the tests on low-calcite material. Therefore, the second reason is perhaps plausible at least for low-calcite material. It is that creep causes high stress concentration areas in the vicinity of pore throats to selectively close. In this case, creep would be expected to reduce permeability more than quasi-elastic deformation.

## 5.2 Long-Term Creep.

A typical result is shown in Figure 18. Duration of this test was about five days. Note that the average creep rate is less than shown for the previous tests. This is expected as duration increases.

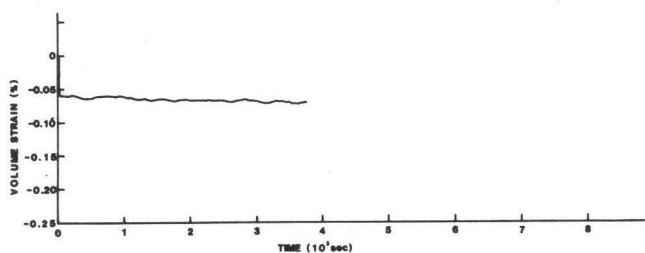


Figure 18. Long-term creep test on material from Cerro Prieto well T-366, creep rate is approximately  $0.3 \times 10^{-9} \text{ sec}^{-1}$ .

## 6. FLUID CHEMISTRY RESULTS.

Analyses of fluid from tests give a good overview of rock-brine interaction during testing. Excluding the results from tests CP-4 and CP-5, where problems with the pore pressure system caused brief occasions of flashing of the fluid to steam in the specimen, sodium, potassium and chloride concentration in the output fluids tend to be quite similar to those in the input

fluids, thus indicating that most residue was cleaned out. The fluids from tests CP-7 and CP-9 show high calcium concentrations, which correspond nicely to the very high calcium carbonate contents in the rock (6-8%  $\text{CaCO}_3$ ). These values emphasize the importance of choosing good rockbrine matches for high temperature testing.

The most critical fluid constituents, from the viewpoint of brine-rock mechanical interactions, are silica, calcium and bicarbonate. Table 8 summarizes the analyses performed for these constituents. Concentration of silica in the output fluid tend to be dependent upon the time the fluid was detained within the rock, as summarized in Figure 19. For the test, excluding CP-4 and CP-5, the analyses of fluids detained for approximately one hour show a loss of silica, which is probably due to a small thermal disequilibrium; however, fluid from tests with detention times greater than one hour, but less than a day, show a large increase of silica. The concentrations reached values as high as 3300 parts per million, which is greater than five times the initial value. These values later drop to values equal to or below original values. (Fluid samples from the Cerro Prieto tests were not filtered, and thus, reported silica values include suspended, colloidal, and dissolved solids). These high values are well in excess of saturation concentration for silica even with respect to amorphous phases, indicating the presence of other chemical, thermochemical or chemical-mechanical effects. The values reported for longer-term testing seem to suggest a return to equilibrium as long-term testing goes on.

Table 8

### Silica and Carbonate Chemistry

Test I.D.	Fluid Detention Time	Silica		Calcium		Bicarbonate		$\text{CaCO}_3$ In Rock
		In	Out	In	Out	In	Out	
CP3	11 Hours	1000	600	--	--	~0	850	1%
CP4*	1 Hour	680	380	300	320	0	180	0%
	6 Hours	680	290	300	280	0	470	0%
CP5*	3 Hours	680	440	300	20	0	340	1%
CP6	1 Hour	620	170	270	660	0	550	0%
	3 Hours	620	3100	270	350	0	800	0%
CP7	3 Hours	620	3300	270	480	0	420	8%
CP8	2 Hours	620	2500	270	230	0	620	0%
CP9	1 Hour	620	590	270	490	0	520	6%
	4 Hours	620	2300	270	640	0	1550	6%

\*The fluid from CP4 and CP5 was flashed before sampling.

The calcium concentration in the pore fluid before and after being introduced to the rock, again excluding tests CP-4 and CP-5, indicate that if any reactions occurred, they were probably related to

the dissolution of calcium carbonate. Since all of the specimens contain some calcium carbonate (values reported as zero indicate less than 0.5%), this type of reaction is expected for calcium concentration that are less than saturation.

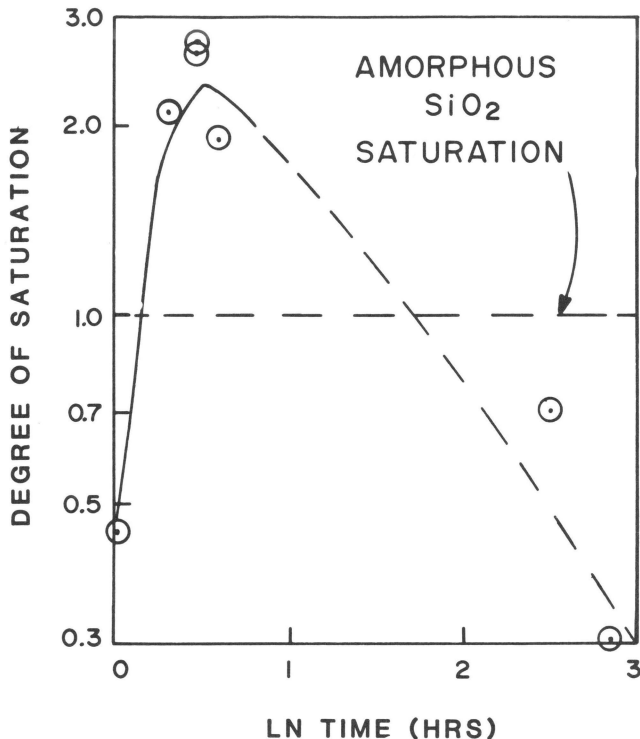


Figure 19. Concentration of silica with respect to degree of saturation for several Cerro Prieto creep tests as a function of time during the tests.

The purpose of this phase of this program were to insure equilibrium with respect to water-rock interactions and to gain insight into any reactions which might be occurring during a test sequence on a rock specimen if equilibrium was not achieved or disturbed by a change in stress state. Analyses of pre- and post-test pore fluid from the tests show that in cases where equilibrium has not been achieved, reactions are probably not of major consequence to short-term mechanical response. Effects are present and include mechanisms such as calcium carbonate dissolution and transportation of suspended silica out of the rock samples.

The suspended silica, in particular, might be one of the best clues we have as to the mechanism of creep compaction in these rocks (when it occurs). For Cerro

Prieto, the solubility of  $\text{SiO}_2$  at test conditions is approximately 400 ppm for quartz and 1200 ppm for amorphous silica. Thus, a consistent picture of results with respect to silica during creep testing is: The increased effective stress caused by reduction of pore pressure causes pressure solution at quartz contact boundaries. This causes a local supersaturation, but with time as initial solution rate and initial creep rate diminish, equilibrium is once again achieved.

## 7. SUMMARY AND SYNTHESIS OF TEST RESULTS.

Core for this testing program was obtained from the Cerro Prieto Geothermal field in order to make measurements at simulated in-situ conditions for the purpose of determining the mechanism of compaction and their relation to surface subsidence. The major rock type tested was sedimentary sandstone. There is ample evidence in this material of hydrothermal alteration. This can be seen, for example, by the high epidote content of much of the rock. Epidote is a product of high temperature alteration which certainly occurs at the 300°C temperature of the Cerro Prieto reservoir.

Essentially, two types of tests were run (with some variations). The so-called basic test began at reservoir conditions and then investigated the effects of changes in pore pressure, confining pressure and ratio of axial stress to confining pressure on the compressibility of specimens. The creep tests began at the same initial conditions as the basic tests and the investigated the effects of reduced pore pressure for long periods of time to determine time-dependent (creep) effects related to compaction. Some permeability measurements were also included with the creep tests.

A summary of basic test results is given in Table 9. Compressibilities range from 0.7 to 0.9 x 10<sup>-6</sup> psi<sup>-1</sup>. These typical compressibilities for normally consolidated sandstones in this porosity range. The Cerro Prieto reservoir materials, in general, were fairly elastic. Ultrasonic velocities were also measured during some of the tests to determine if these velocities were sensitive to compaction, for possible use as a field indicator of compaction. Indeed, a sensitivity was measured, as shown in the Table 6. This is consistent with compaction-caused density increase. However, the small increase in velocity of about one percent is of uncertain usefulness as a diagnostic indicator in the field.



Table 9

Basic Tests  
Average ResultsCompressibility ( $10^{-6}$  psi $^{-1}$ )

Test Type	Stress Difference	Cerro Prieto Reservoir
$\Delta P_p$	Low	0.7
	Intermediate	0.7
	High	Shear failure
$\Delta P_c$	Intermediate	0.9
$\Delta P_p$ Uniaxial	Intermediate	0.8

A summary of creep test results is shown in Table 10. Creep test duration varied from about 0.2 to  $4 \times 10^5$  seconds. This covers a range of a few hours to greater than 5 days. In general,

Table 10

Creep Tests  
Average Results

	Average Duration ( $10^5$ /sec)	Average Rate ( $10^{-9}$ /sec)	Range of Rates ( $10^{-9}$ /sec)
Cerro Prieto Short Term	0.2	7.2	1.7 - 87.0
Cerro Prieto Long Term	4.0	0.3	---

creep rates on the order of  $1 \times 10^{-9}$  per second were observed, measured as rate of change in volume strain. At this creep rate, were it steady, all porosity would be entirely removed from these rocks in a few years. However, it is unlikely that this reduction rate could continue at steady-state. Instead, the reduction would likely increase when a new equilibrium value of porosity was achieved. Viewing the creep results in more detail, we see that the apparent creep rate decreases as the duration of the test increases. This supports the observation that the creep compaction here is probably not at steady state and is tending toward a new equilibrium value of porosity. However, none of the tests were carried to sufficient duration to experimentally confirm this supposition, and it would be impractical to test rocks for the many

months necessary to do this. Instead, we must turn to a theory based on mechanisms in order to extrapolate results to long periods of time, and use the experiments to provide an initial creep rate only.

Comparing the results for all rocks, we see that creep rate tended to decrease with increasing grain size and decrease with decreasing porosity. One specimen exhibited extremely high creep rate (almost two orders of magnitude greater than the average). It was a relatively unconsolidated fine-grained specimen. The high temperature of the Cerro Prieto reservoir did not in itself result in a high measured creep rate in this rock. On the contrary, the mineralogical state of the Cerro Prieto specimens that are most highly hydrothermally altered may even inhibit creep. This is possibly explained by the acceleration of in-situ mechanisms that result in cementation and reduction of stress concentrations in hydrothermally altered material so that the rock is already stable in a high-temperature stressed environment. It follows that less-altered sediments, as seen in some of these rocks, are more susceptible to perturbations from their natural state. This observation is consistent with normal views of sedimentary and metamorphic processes in rocks.

In summary, we have observed that compaction is time-dependent in most of the rocks we have observed. For a 1,000 psi reduction in pore pressure. The instantaneous volume strain associated with compaction (for a compressibility of about  $1 \times 10^{-6}$  psi) is about  $1 \times 10^{-3}$ . Typically, the creep we have observed would double this volume strain in about one day and increase it by a factor of ten in about three months, assuming a long-term creep rate of about  $1 \times 10^{-9}$  per second. This means that in three months time the apparent compressibility with respect to pore pressure reduction is one order of magnitude greater than that which would be measured by ordinary laboratory techniques.

Fluid chemistry as measured in all of these specimens, for both input and output fluids, has been controlled to minimize the effect of non-equilibrium reactions otherwise caused by use of improper test fluid. This is particularly important at the elevated temperatures of these tests. As an indicator of chemical/mechanical effects that may relate to possible mechanisms of creep compaction, silica analysis has been most useful. During the earlier phases of creep testings, the silica content of output fluids increases to levels beyond those of saturation. However, for later phases of creep testings, silica

concentrations trend back toward values that are consistent with equilibrium. This could indicate possible mechanisms of pressure solution at asperity contact between quartz grains. At these points quartz would be driven rapidly into solution and could easily exceed equilibrium values for the solution at its own pressure and temperature. Then, with time, the excess quartz in solution would have to come out of solution, most likely as euhedral quartz in areas where stress concentrations are absent. This has certainly been observed as a mechanism of diagenesis in sandstone sedimentary sequences. We have perhaps only accelerated the process by the increase in effective stress during our tests. Some confirming evidence of this is found in the SEM results on post-test material.

Permeability values obtained for Cerro Prieto material, as shown in Table 7 indicate an average initial permeability of about 4 millidarcies. This permeability is lower than that determined from field tests at the reservoir. This would indicate that flow, on average, in this geothermal reservoir must be through channels of higher permeability or fractures, or both. This is certainly conceivable, considering the tectonically active nature of the area. With temperature increase, we observed a 40% decrease of permeability, but with pore pressure decrease we observed no statistically significant change in permeability. With creep we observe a further 39% reduction in permeability. It is interesting to note that creep has a more significant effect on permeability than on compressibility. This could be associated with creep compaction mechanisms that are active at asperity positions, which would possibly be very near to pore throats, therefore causing an amplifying effect. This conclusion, however, must be considered to be very preliminary, since other mechanisms of permeability reduction such as particulate plugging, could also be active here.

In general, the testing done on this program has indicated that rocks from the Cerro Prieto reservoir behave more or less as normally consolidated sandstones in short-term response. However, in long-term response the rocks exhibited a creep tendency that is most pronounced in the less consolidated, less hydrothermally altered material. The amount of creep is sufficient to cause the amount of compaction over a period of months or years to be one to two orders of magnitude greater than initial compaction related to instantaneous quasi-elastic behavior.

## 8. CONCLUSIONS AND IMPLICATIONS FOR SUBSIDENCE PREDICTION.

This program has demonstrated that rocks from the Cerro Prieto geothermal field behave quite normally with respect to instantaneous compaction as caused by pore pressure reduction, having compressibilities of the order  $10^{-6}$  psi. They also demonstrate a tendency to compact further with time. The rate of creep compaction varies from rock to rock, or of the order  $10^{-9}$  sec<sup>-1</sup> and is statistically significant. The creep results are consistent with a theory of creep compaction developed here (Schatz and Carroll, 1981 and Schatz, 1982) that is based on spherical pore analysis and previous work on pressure solution in quartz sandstones.

Test results show that for a typical 1000 psi reduction in pore pressure, similar to that caused by reservoir production, a compaction strain of 0.001 can be expected to be observed instantaneously. However, for a creep rate of  $1 \times 10^{-9}$ /sec, an ultimate compaction of about 0.03 in a time period of a few years can be expected. These results are approximate and are based on theoretical extrapolation. Nevertheless, this ultimate compaction is a factor of 30 greater than the initial compaction. An alternative statement of this result is that the ultimate effective long-term compressibility is about  $30 \times 10^{-6}$  psi rather than  $1 \times 10^{-6}$  psi.

According to the theory developed here, the magnitude of ultimate creep compaction is a function mainly of initial porosity and pore pressure drop and not a strong function of rock type. (It is important to note that we have assumed a normally consolidated rock, that is, one that has not previously experienced a higher effective stress than it currently experiences in the reservoir, and a non-highly cemented rock. Preconsolidated rock or highly cemented rock will probably show less tendency to creep compact). On the other hand, the rate of creep compaction is a function mainly of the pressure solution rate, and is therefore strongly dependent upon grain type, temperature, grain contact angularity, cementation that would reduce stress concentrations, etc. However, even accounting for our uncertain knowledge of the values of parameters, we find that an initial creep compaction rate on the order  $10^{-9}$  sec<sup>-1</sup> should be common for fairly clean, normally consolidated sandstones. Extremely angular-grained, small-grained and high porosity sands would be expected to have a higher initial creep rate.

As a result of the experimental and theoretical analyses performed during this program, we conclude that the difference between laboratory measured and field-measured moduli that is usually attributed to size effect (certainly some part of this is truly size effect) may to some extent be attributable to time-dependent creep phenomena that are not ordinarily observed in the laboratory because of the short term nature of most laboratory tests. Unfortunately, it would not be practical to routinely test rock for periods of months; however, it is suggested that when a large suite of rocks is being tested, and accurate moduli values are very important, that at least a few of these rocks be tested for creep effects.

Consider, for example, the effect on the compaction of a subsurface reservoir, leading to subsidence. For a reservoir thickness of 100 meters and a pore pressure reduction of 1000 psi, the instantaneous compaction-related thickness loss predicted by results here might be approximately 10 centimeters. If this were all the compaction to occur, it would be expected to be translated to the surface as an ultimate subsidence of a few centimeters at most. However, with the occurrence of creep, an ultimate compaction of 30 times this amount might occur. The compaction thickness loss is now 300 centimeters, and the surface subsidence resulting from this might be a few tens of centimeters, which, depending upon location, might be significant.

#### 9. ACKNOWLEDGEMENTS.

Many people have contributed to the success of this project. We thank especially: from the Earth Science Division of the Lawrence Berkeley Laboratory - J. Noble, T.J. Narisimhan, S. Vonderhaar, M. Lippman, and N. Goldstein; from the Comisión Federal de Electricidad - Ing. A. Mañón M.;

from the Mechanical Engineering Department of the University of California at Berkeley M. Carroll; from the Terra Tek, Inc. Professional staff - K. Wolgemuth, A.S. Abou-Sayed, S. Carlisle, M. Smith, R. Van Buskirk, and S. Kelkar; and from the Terra Tek support staff - R. Binch, L. Beard and A. MacLeod.

#### 10. REFERENCES

- Elders, W.A., Jr., Hoagland, J.R., Olson, E.R., McDowell, S.D. and Collier, P., "A Comprehensive Study of Samples from Geothermal Reservoirs: Petrology and Light Stable Isotope Geochemistry of Twenty-Three Wells in the Cerro Prieto Geothermal Field, Baja California, México," Institute of Geophysics and Planetary Physics, University of California, Riverside, 1978.
- Elders, W.A., ed., Guidebook, "Geology and Geothermics of the Salton Trough," Geological Society of America 92nd Annual Meeting, San Diego, 1979.
- Grimsrud, G.P., Turner, B.L. and Frame, P.A., "Areas of Ground Subsidence Due to Geofluid Withdrawal," Geothermal Subsidence Research Management Program, Lawrence Berkeley Laboratory, 1978.
- Reed, M.J., "Geology and Hydrothermal Metamorphism in the Cerro Prieto Geothermal Field, México," Proceedings, Second U.N. Symposium on Development and Use of Geothermal Resources, 1, 539-547, 1976.
- Schatz, J.F. and Carroll, M.M., "Creep Compaction of Porous Rock," in Proc. Intl. Symposium on Weak Rock, Tokyo, 1981.
- Schatz, J.F., "Physical Processes of Subsidence in Geothermal Reservoirs," Terra Tek Report TR 82-39, Terra Tek Research, Salt Lake City, 1982.